Vol. 2 (1) (2021)

Measurement, Control, and Automation

Website: https:// mca-journal.org

ISSN 1859-0551

Modeling and Control of a Novel Structure of the 4DOF-Hybrid Magnetic Bearings
Mô Hình Hóa và Điều Khiển Cho Cấu Trúc Mới Của Ổ Từ Kiểu Lai 4 Bậc Tự Do

Vũ Đình Đạt[1], Nguyễn Quang Địch[1,*], Nguyễn Huy Phương[1]
[1] Hanoi University of Science and Technology, Hanoi, Vietnam
[*] Corresponding author email: dichnq@gmail.com

Abstract

This paper presents the modeling and control of a Novel Structure of the four Degrees of Freedom (4DOF) Hybrid Magnetic Bearings (HBMs) with a rigid rotor. In which, the centralized PD control is applied to control the HBM at its center coordinates. First, the magnetic force is calculated through the equivalent magnetic circuit, the position stiffness and the current stiffness are identified by linearizing around the operating space. From there, the mathematical model of the HMB is introduced. The dynamic properties of the parallel and inclination mode of the rotor were analyzed to design a centralized PD controller. Finally, the proposed control strategy was verified by simulation. The results indicate that the HBM not only works stably but also ensures independent control of the rotor's translation and inclination.

***Keywords**: Active magnetic bearing, Hybrid magnetic bearing, Centralized PD controller, Center of gravity coordinates of rotor*

Symbols

Symbols	Units	Description
Φ	Wb	Bias flux
H	A/m	Magnetic field strength
B	Tesla	Flux density
F	N	Magnetic motive force
I	A	Current in coil
x	mm	Air gap length
R	Ω	Reluctance

Abbreviations

FEM	Finite Element Method
EMCM	Equivalent Magnetic Circuit Method
PMB	Passive Magnetic Bearing
AMB	Active Magnetic Bearing
HMB	Hybrid Magnetic Bearing
PD	Proportional Derivative Controller

Tóm tắt

Bài báo này giới thiệu phương pháp xây dựng mô hình toán học và thiết kế hệ điều khiển cho một cấu trúc mới của ổ từ 4 cực kiểu lai có rotor nguyên khối. Trong đó bộ điều khiển PD tập trung được thiết kế theo hệ tọa độ trọng tâm để điều khiển ổ từ. Đầu tiên, lực nâng sẽ được tính toán thông qua phương pháp mạch từ tương đương, độ cứng vị trí và độ cứng dòng điện được xác định thông qua phương pháp tuyến tính hóa xung quanh điểm làm việc của ổ từ. Từ đó mô hình toán học của ổ từ kiểu lai sẽ được đề xuất. Đặc tính động học của ổ từ được phân tích trong các chế độ rotor di chuyển song song và nghiêng để hỗ trợ thiết kế bộ điều khiển PD tập trung tại hệ tọa độ trọng tâm. Để kiểm chứng khả năng hoạt động của ổ từ kiểu lai với phương pháp điều khiển được đề xuất, phần cuối bài báo sẽ trình bày về phương pháp mô phỏng dựa trên Matlab/Simulink. Các kết quả mô phỏng chỉ ra rằng, ổ từ không những làm việc ổn định mà còn đảm bảo điều khiển độc lập được di chuyển của rotor trong các chế độ tịnh tiến và xoay nghiêng.

1. Introduction

Nowadays, magnetic bearings are specially noted for their many advantages such as no friction, no lubrication and less maintenance. Therefore, they are widely used in turbines, high-speed spindles, and flywheels in satellites, etc. [1,2]. In all types of magnetic bearings, hybrid magnetic bearings (HMBs) are increasingly being noticed by the advantages that other magnetic bearings do not have. Instead of only the electromagnetic force in the coil as in the active magnetic bearings (AMBs), the hybrid magnetic bearing has more electromagnetic force generated by permanent magnets. As the result, the HMB has higher efficiency and higher stiffness than those of the AMB and passive magnetic bearings (PMBs) [3,4]. Consequently, high precision control can be achieved. Various structures for HMBs have been proposed [5,6]. In which, the bias flux and the control flux share the same paths. This will lead to large control of current due to large permanent magnet reluctance, thus power loss is high. In addition, there are other structures for HMBs, which produces radial and axial force. The bias flux and the

Received: 17 May 2021; Accepted: 15 June 2021.

control flux go through the laminated rotor. Consequently, a lot of magnetic motive force (MMF) is lost, and the volume of permanent magnet will be large. A more simplified structure for radial HMB is given in [7,8]. The bias flux is separated from the control flux, nevertheless, extra radial force can be produced to generate the coupling force between radial and axial directions. As a result, the control process is more complex, and the structure is not fit for the integrated unit.

Moreover, the other problems of the above HMBs are coupled between magnetic circuits of X and Y channels or bias flux and the control flux share the same path. They will let more difficult to design control systems and cause high loss.

A novel structure for a radial HMB is introduced in this paper in which magnetic circuits of X and Y channels are almost independent of each other, and a gap to separate the magnetic field is introduced to increase the path for the control flux. The mathematical model of the HBM is analyzed in detail. Then, a method of centralized PD control was designed on the basis of a simplified linear model for the rotor shaft using the rotor'center coordinates. Finally, the simulation by the Simulink/Matlab is conducted to verify the proposed control method for HBM.

2. Dynamic analysis of HMB system

2.1. System structure

The structure of the adopted 4-DOF HBM system is depicted in Fig.1.

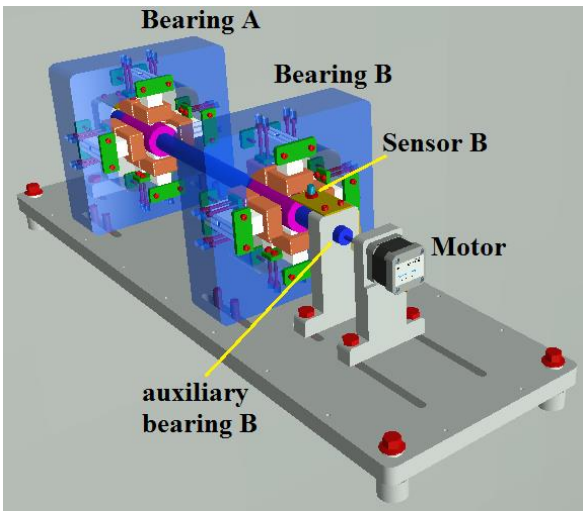

Fig. 1. Structure of 4-DOF HMB system.

Two HBMs A and B are used to support the rotor and limit the 4 degrees of freedom of translational and rotational motion in the X and Y axes. The rigid rotor is transmitted by rotational motion via a motor with a soft coupling. The flexible coupling also limits the axial motion of the rotor. Eddy current sensing systems are mounted on both sides to determine the rotor distance in the X and Y axis directions. In addition, the system also integrates two auxiliary bearings to support the rotor when the system is not operating and also prevents the rotor from contacting the polarity of the magnetic bearings.

Hybrid Magnetic bearing A and B have exactly the same structure and size Fig.2. On each magnetic bearing attach 4 magnetic poles that are symmetrical and evenly spaced to create an attractive force that pushes the rotor in the X and Y axes.

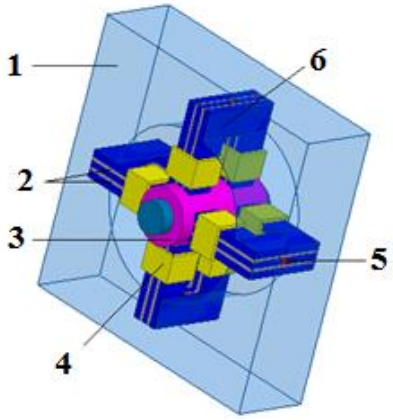

1- magnetic bearing frame, 2- non-magnetic gap

3-rotor iron, 4-coil, 5-permanent magnet, 6-stator iron

Fig. 2. Structure of 4-DOF HMB system.

For more clarity, we will show the details of a magnetic pole as shown in Fig.3. The new hybrid magnetic pole consists of two main parts, the middle part is fitted with permanent magnets and the outer part is separated by non-magnetic gap.

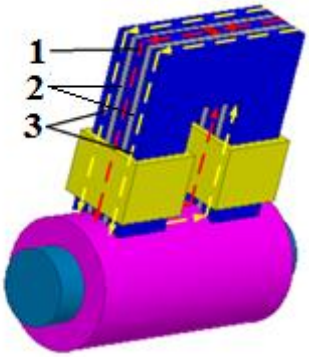

1-middle part, 2-outer part, 3- non-magnetic gap

Fig. 3. Magnetic Pole Structure.

With this structure, the flux path of the control coil and the magnetic flux path of the permanent magnet have been expanded and not limited by the permanent magnet. Furthermore, the non-magnetic gap reduces the flux loss of permanent magnets. The advantages of the novel hybrid magnetic bearing structure are to enhance the magnetic force, reducing the flux loss and increasing the amplitude of control by the increased magnetic saturation limit of the magnetic poles.

2.2. Magnetic force

Because of the symmetry and uniformity of the magnetic poles in a magnetic bearing, we will analyze the magnetic force acting on the rotor in the x-axis direction and from that deducing the magnetic force in the y-axis will be

similar. Assume that the rotor moves up in the positive direction of the X-axis by a distance x (Fig.4).

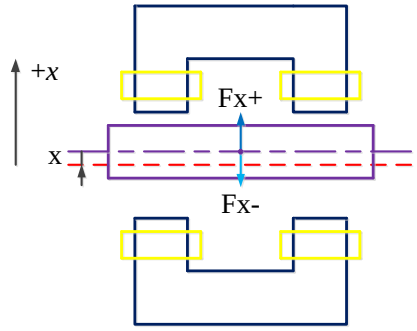

Fig. 4. Rotor moves up by a distance x in the direction (+x).

The flux in the magnetic pole is divided into two parts, the first part passes through the middle part of the magnetic pole with permanent magnet Øi and the second part passes through the outer part of the magnetic pole without permanent magnet Øo. Equivalent magnetic circuit of each part in Fig.5 and Fig.6.

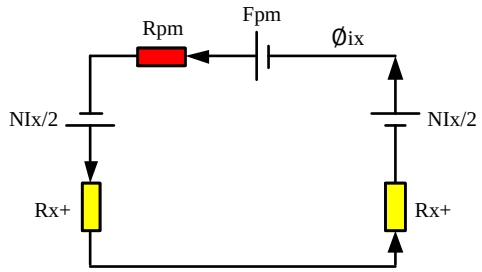

Fig. 5. Equivalent magnetic circuit of the middle part of the magnetic pole.

F_{pm} is the magnetic motive force of the permanent magnet.

NIx/2 magnetic motive force of the control coils.

R_{pm} is the reluctance of the permanent magnet, R_{x+} is the reluctance of the permanent magnet of the air gap between the magnetic pole and the rotor.

Total reluctance of the equivalent magnetic circuit:

$$R_{ix} = R_{pm} + 2R_{x+} = R_{pm} + \frac{2\ x_0 - x}{\mu_0 A_i} \qquad (1)$$

A_i is the area of the inner cross-section that contains permanent magnets. $A_i = k_i A$ with A is the total area of the pole cross-section from the air gap to the rotor.

$$R_{ix} = R_{pm} + \frac{2\ x_0 - x}{\mu_0 k_i A} \qquad (2)$$

Bias fluxes the equivalent magnetic circuit:

$$\phi_{ix} = \frac{F_{pm} + NIx}{R_{ix}} = \frac{F_{pm} + N(i_0 + i_x)}{R_{ix}} \qquad (3)$$

N is the total number of turns of the two windings on both sides of the magnetic pole. i_{0x} is the control current at the position where the rotor lies in the middle balance, i_x is the amount of change in the control current when the rotor moves up by a distance x.

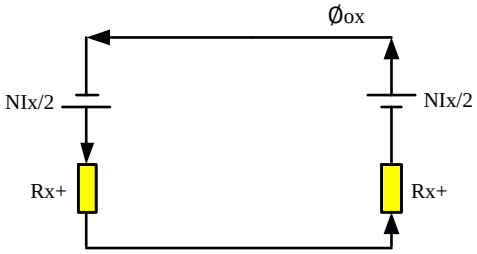

Fig. 6. Equivalent magnetic circuit of the outer part has no permanent magnets.

Total reluctance of the equivalent magnetic circuit:

$$R_{ox} = 2R_{x+} = \frac{2\ x_0 - x}{\mu_0 A_o} \qquad (4)$$

A_o - the area of the outer part has no permanent magnets, $A_o = k_o A$.

$$R_{ox} = \frac{2\ x_0 - x}{\mu_0 k_o A} \qquad (5)$$

Bias fluxes - the equivalent magnetic circuit:

$$\phi_{ox} = \frac{NIx}{R_{ox}} = \frac{N(i_0 + i_x)}{R_{ox}} \qquad (6)$$

Magnetic force of the upper magnetic pole exerted on the rotor is equal to the total magnetic force generated by the magnetic flux between the magnetic pole containing the magnet and the outer part. According to the principle of virtual work, the magnetic force is calculated as follows:

$$F_{x+} = \frac{2\phi_{ix}^2}{\mu_0 A_i} + \frac{2\phi_{ox}^2}{\mu_0 A_o} \qquad (7)$$

Substituting (2), (3) and (5), (6) into (7) written:

$$F_{x+} = \frac{2\mu_0 k_i A\left[F_{pm} + N\ i_0 + i_x\right]^2}{\left[\mu_0 k_i A R_{pm} + 2\ x_0 - x\right]^2} + \frac{\mu_0 k_o A\ N(i_0 + i_x)^2}{2\ x_0 - x^2} \qquad (8)$$

Performing the same calculations, we can determine the magnetic force of the magnetic pole below acting on the rotor:

$$F_{x-} = \frac{2\mu_0 k_i A\left[F_{pm} + N\ i_0 - i_x\right]^2}{\left[\mu_0 k_i A R_{pm} + 2\ x_0 + x\right]^2} + \frac{\mu_0 k_o A\ N(i_0 - i_x)^2}{2\ x_0 + x^2} \qquad (9)$$

Total magnetic force exerted on the rotor in the x-axis direction:

$$F_x = F_{x+} - F_{x-} \qquad (10)$$

Substituting (8), (9) into (10) and then linearizing the formula (10), the following linearized equation can be derived:

$$F_x \approx \frac{\partial F_x}{\partial i_x}\Big|_{\substack{i_x=0\\x=0}} i_x - \frac{\partial F_x}{\partial x}\Big|_{\substack{i_x=0\\x=0}} x \qquad (11)$$

The first and second coefficients of equation (11) are the current stiffness Ki and radial displacement stiffness Kx of the HMB respectively given by

$$K_i = \frac{8\mu_0 k_i AN\ \ F_{pm} + Ni_0}{\mu_0 k_i AR_{pm} + 2x_0}^2 + \frac{2\mu_0 k_o AN^2 i_0}{x_0^2} \quad (12)$$

$$K_x = -\frac{16\mu_0 k_i A\ \ F_{pm} + Ni_0}{\mu_0 k_i AR_{pm} + 2x_0}^2 - \frac{2\mu_0 k_0 A\ \ Ni_0}{x_0^3}^2$$

(13)

So the linearization equation of the magnetic force in the direction of the x-axis is determined as follows:

$$F_x \approx K_i i - K_x x \qquad (14)$$

The current stiffness Ki and radial displacement stiffness Kx display the axial load bearing capacity and the stability of the hybrid magnetic bearing.

2.3. System modelling

The schematic of a 4-DOF HMB system is shown in Fig.7.

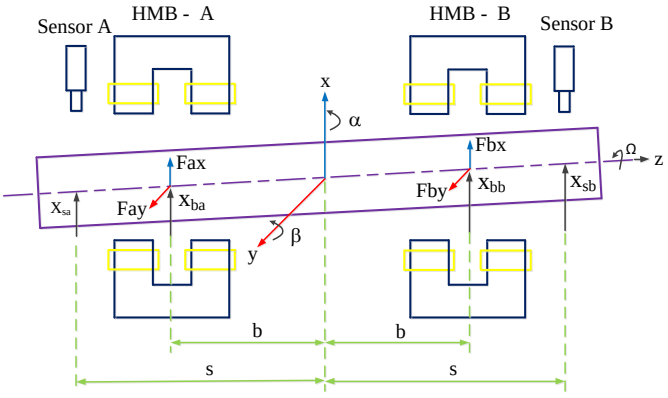

Fig. 7. Model of magnetically suspended rotor system.

Select the coordinate system at the center of the Rotor (COD), the movement of the Rotor will include the translational motion of the center mass (x, y) and the rotation with Euler angles (α, β). The dynamic model of 4-DOF HMB rotor system can be described as

$$M\ddot{q} + G\dot{q} = Bf \qquad (15.1)$$

$$q_s = Tq \qquad (15.2)$$

Where, $q = \beta \quad x \quad \alpha \quad y^T$ is the coordinate of the rotor center; $q_s = x_{sa} \quad x_{sb} \quad y_{sa} \quad y_{sb}^T$ is the rotor displacement at the sensor position; M is the mass matrix; G is the gyroscopic matrix; $f = \begin{bmatrix} f_{ax} & f_{bx} & f_{ay} & f_{by} \end{bmatrix}^T$ is the active control forces of HMBs, and B and T are transformation matrices.

$$M = \begin{bmatrix} I_y & 0 & 0 & 0 \\ 0 & m & 0 & 0 \\ 0 & 0 & I_x & 0 \\ 0 & 0 & 0 & m \end{bmatrix} \quad G = \begin{bmatrix} 0 & 0 & I_z\Omega & 0 \\ 0 & 0 & 0 & 0 \\ -I_z\Omega & 0 & 0 & 0 \\ 0 & 0 & 0 & 0 \end{bmatrix}$$

$$B = \begin{bmatrix} -b & b & 0 & 0 \\ 1 & 1 & 0 & 0 \\ 0 & 0 & -b & b \\ 0 & 0 & 1 & 1 \end{bmatrix} \quad T = \begin{bmatrix} -s & 1 & 0 & 0 \\ s & 1 & 0 & 0 \\ 0 & 0 & -s & 1 \\ 0 & 0 & s & 1 \end{bmatrix}$$

From equation (14) deduce

$$f = \begin{bmatrix} k_{ai} & 0 & 0 & 0 \\ 0 & k_{bi} & 0 & 0 \\ 0 & 0 & k_{ai} & 0 \\ 0 & 0 & 0 & k_{bi} \end{bmatrix} \begin{bmatrix} i_{ax} \\ i_{bx} \\ i_{ay} \\ i_{by} \end{bmatrix} - \begin{bmatrix} k_{as} & 0 & 0 & 0 \\ 0 & k_{bs} & 0 & 0 \\ 0 & 0 & k_{as} & 0 \\ 0 & 0 & 0 & k_{bs} \end{bmatrix} \begin{bmatrix} x_{ba} \\ x_{bb} \\ y_{ba} \\ y_{bb} \end{bmatrix}$$

$$f = \begin{bmatrix} f_{ax} \\ f_{bx} \\ f_{ay} \\ f_{by} \end{bmatrix} = K_i i - K_s q_b \qquad (16)$$

The vector $q_b = x_{ba} \quad x_{bb} \quad y_{ba} \quad y_{bb}^T$ is the rotor displacement at the HMB positions.

The vector $i = \begin{bmatrix} i_{ax} & i_{bx} & i_{ay} & i_{by} \end{bmatrix}^T$ is the individual coil control currents of HMBs.

By combining (15) and (16) we obtain the following basic equation of motion for the rotor to be levitated by HMBs:

$$M\ddot{q} + G\dot{q} = B(K_i i - K_s q_b) \qquad (17.1)$$

$$q_s = Tq \qquad (17.2)$$

$$q_b = \begin{bmatrix} x_{ba} \\ x_{bb} \\ y_{ba} \\ y_{bb} \end{bmatrix} = \begin{bmatrix} -b & 1 & 0 & 0 \\ b & 1 & 0 & 0 \\ 0 & 0 & -b & 1 \\ 0 & 0 & b & 1 \end{bmatrix} \begin{bmatrix} \beta \\ x \\ \alpha \\ y \end{bmatrix} \qquad (18.1)$$

$$q_b = B^T q \qquad (18.2)$$

By insertion of (18) into (17), one obtains the following differential equation at coordinates of the rotor center:

$$M\ddot{q} + G\dot{q} + BK_s \mathrm{B}^T \mathrm{q} = BK_i i \qquad (19.1)$$

$$M\ddot{q} + G\dot{q} + K_{ns}\,\mathrm{q} = BK_i i \qquad (19.2)$$

Where, $K_{ns} = BK_s B^T$ is the transformed negative bearing stiffness matrix.

K_{ns} matrix is symmetrical through the following proof:

$$K_{ns}^T = (BK_s B^T)^T = BK_s^T B^T = BK_s B = K_{ns}$$

$$K_{ns} = \begin{bmatrix} k_{as}b^2 + k_{bs}b^2 & -k_{as}b + k_{bs}b & 0 & 0 \\ -k_{as}b + k_{bs}b & k_{as} + k_{bs} & 0 & 0 \\ 0 & 0 & k_{as}b^2 + k_{bs}b^2 & -k_{as}b + k_{bs}b \\ 0 & 0 & -k_{as}b + k_{bs}b & k_{as} + k_{bs} \end{bmatrix}$$

(20)

$K_s^{\,T} = K_s$ because is the diagonal matrix.

We find that the matrices to the left of (19.2) have their dedicated symmetry properties. As can be seen, the mass matrix M is symmetrical; the gyroscopic matrix G is skew-symmetrical; the transformed negative bearing stiffness matrix K_{ns} is also symmetrical. Based on such characteristics, it can be observed that the system is highly stable and controllable.

3. PD-Control Design

3.1. Magnetic bearing control overview

Control methods contribute an important role in designing a magnetic bearing system. These include conventional decentralized approaches such as PD, PID for each bearing unit and separately for each bearing axis [9]. However, local PD or PID control can also lead to problems when the performance of a controller is highly influenced by the coupled impact in motion of the magnetic bearing system. In the centralized methods, there is a lot of research about the state feedback control techniques can be considered. As the full system state including the velocities is usually not directly measured in a standard rigid body magnetic bearing system, the only choice will be an observer or state estimator based on control design approach such as LQG-control [10, 11]. In the case of a rigid rotor magnetic bearing system, it can be shown, however, that these methods do not feature appreciable advantages over decentralized [11]. Apart from problems due to uncertainties in the dynamics of the state estimator LQG-control even features a potential for destabilization of the closed-loop magnetic bearing system with the with variable rotational speed. The closed-loop system will behave nicely at the design speed, but most probably it will become unstable at other speeds. Other than the above mentioned estimator based state feedback control techniques, the modern H∞ or μ−synthesis control design concepts [12, 13, 14] are much more promising for the use in AMB applications, in particular for elastic rotors. For pure hard rotor control, these methods do not give much better results than those obtained with the parallel / conical control mode using the COG coordinates since the structure of the feedback matrices obtained with H∞ or μ−synthesis control will not be fundamentally different from what is achievable with COG coordinate control.

Therefore, an enhanced control structure is introduced here, which, on the one hand, solves both shortcomings of decentralized control shown above and, on the other hand, implements MIMO control while keeping the possibility for interpreting feedback parameters as physical quantities in a single-input-single-output (SISO) like way, similarly to local feedback. This control structure makes use of the physical effect that the parallel and conical modes of the rigid body plant are decoupled. By transforming the controller input signals in such a way that the parallel and conical modes can be detected separately. The control output signals, physically corresponding to the moment of force with respect to the rotor's center of gravity S and to the concentrated force in S, must then only be transformed into suitable forces in the bearing A and B. In this way, method of centralized PD control of the rigid rotor is achieved. The idea of this control structure is shown in Fig.8.

3.2. Centralized PD control

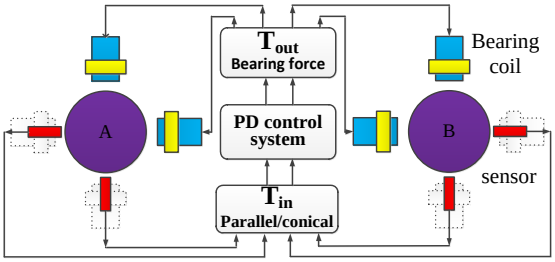

Fig. 8. Feedback structure for decoupled control of parallel / conical modes.

Starting from equation (14):

$$M\ddot{q} + G\dot{q} + K_{ns}\,\mathrm{q} = BK_i i$$

We build PD type feedback law which utilizes the center of gravity displacements rather than the sensor coordinates by involving the transformation matrix T_{in}. At the output side the transformation matrix, T_{out} has to be applied for the recomposition of the bearing forces or currents respectively:

$$i = -T_{out}PT_{in}q_s - T_{out}DT_{in}\dot{q}_s \qquad (21.1)$$

$$P = diag(P_{co}, P_{pa}, P_{co}, P_{pa}) \qquad (21.2)$$

$$D = diag(\mathrm{D}_{co}, \mathrm{D}_{pa}, \mathrm{D}_{co}, \mathrm{D}_{pa}) \qquad (21.3)$$

$$q_s = \begin{bmatrix} x_{sa} & x_{sb} & y_{sa} & y_{sb} \end{bmatrix}^T \qquad (21.4)$$

$$q = T_{in}q_s = T^{-1}q_s \qquad (22.1)$$

$$T_{in} = T^{-1} = \begin{bmatrix} -s & 1 & 0 & 0 \\ s & 1 & 0 & 0 \\ 0 & 0 & -s & 1 \\ 0 & 0 & s & 1 \end{bmatrix}^{-1} = \frac{1}{2s}\begin{bmatrix} -1 & 1 & 0 & 0 \\ s & s & 0 & 0 \\ 0 & 0 & -1 & 1 \\ 0 & 0 & s & s \end{bmatrix}$$

(22.2)

Substituting (20.1) into (14),

$$M\ddot{q} + G\dot{q} + K_{ns}\,\mathrm{q} = -BK_iT_{out}PT_{in}q_s - BK_iT_{out}DT_{in}\dot{q}_s$$

(23)

Looking at the right side of equation (23), the component PT_{in} and DT_{in} are the diagonal matrix, so to decompose the control force into the component forces that have a separate impact on the translational and conical motion of the rotor, choose the following condition:

$$-BK_iT_{out} = I \qquad (24.1)$$

$$T_{out} = K_i^{-1}B^{-1} = \frac{1}{k_{ai}(2b)}\begin{bmatrix} -1 & b & 0 & 0 \\ \frac{k_{ai}}{k_{bi}} & b\frac{k_{ai}}{k_{bi}} & 0 & 0 \\ 0 & 0 & -1 & b \\ 0 & 0 & \frac{k_{ai}}{k_{bi}} & b\frac{k_{ai}}{k_{bi}} \end{bmatrix}$$

(24.2)

With (24.1), the total closed-loop matrix differential equation for the rigid rotor in HMBs system with the COG coordinate control can be written as follows:

$$M\ddot{q} + G\dot{q} + K_{ns}q + IPq + ID\dot{q} = 0 \qquad (25.1)$$

$$M\ddot{q} + G\dot{q} + K_{ns}q + Pq + D\dot{q} = 0 \qquad (25.2)$$

We can be seen in (25.2) the generally non-diagonal matrix K_{ns} , introduced by the negative stiffness of each magnetic bearing, destroys the decoupling. Only in case of a fully symmetric HMB system with identical bearings on each side the negative stiffness matrix K_{ns} , described by (20), will also be diagonal, and an ideally decoupled system will result. Hence, the control law for the currents must be augmented by a compensation term as follows:

$$i = -T_{out}PT_{in}q_s - T_{out}DT_{in}\dot{q}_s - K_{nscom}q_s \quad (26.1)$$

with the conditions:

$$K_{ns}q = -BK_iK_{ns-}q_s = -BK_iK_{nc-}Tq \quad (26.2)$$

$$K_{ns-} = -K_i^{-1}B^{-1}K_{ns}T^{-1} = -T_{out}K_{ns}T_{in} \quad (26.3)$$

Substituting (20), (22.2), (24.2) into (26.2) gives:

$$K_{nscom} = \frac{-1}{2s}\begin{bmatrix} \frac{k_{as}}{k_{ai}}(s+b) & \frac{k_{as}}{k_{ai}}(s-b) & 0 & 0 \\ \frac{k_{bs}}{k_{bi}}(s-b) & \frac{k_{bs}}{k_{bi}}(s+b) & 0 & 0 \\ 0 & 0 & \frac{k_{as}}{k_{ai}}(s+b) & \frac{k_{as}}{k_{ai}}(s-b) \\ 0 & 0 & \frac{k_{bs}}{k_{bi}}(s-b) & \frac{k_{bs}}{k_{bi}}(s+b) \end{bmatrix}$$

(26.4)

The component $K_{ns}q$ in equation (25.2) has been reduced. Now, the total closed-loop matrix differential equation for the rigid rotor in the HMBs system with the COG coordinate control can be written as follows:

$$M\ddot{q} + G\dot{q} + Pq + D\dot{q} = 0 \qquad (27)$$

So we have built the equations control that the parallel and conical modes separately. The controller is built based on steps of solving 2nd order linear homogeneous differential equation with constant coefficients (27).

Set the sub variables:

$$y_1 = q \ ; y_2 = \dot{q} \ ; \ y = \begin{bmatrix} y_1 \\ y_2 \end{bmatrix} \qquad (28.1)$$

Deduced:

$$\dot{y}_1 = y_2 \qquad (28.2)$$

$$\dot{y}_2 = -M^{-1}((G+D)y_2 + Py_1) \qquad (28.3)$$

State equation of the system:

$$\dot{y} = \begin{bmatrix} \dot{y}_1 \\ \dot{y}_2 \end{bmatrix} = \begin{bmatrix} 0 & I \\ -M^{-1}P & -M^{-1}(G+D) \end{bmatrix}\begin{bmatrix} y_1 \\ y_2 \end{bmatrix} \quad (28.4)$$

$\dot{y} = Ay$ with is state space matrix.

The characteristic equation for its eigenvalues λ:

$$\det(\lambda I - A) = 0 \qquad (28.5)$$

4. Simulation results

In this section, a simulation study is carried out to investigate the effects of the parallel and conical motion modes, the gyroscope effect with the different rotation speeds of the rotor. Simulation is performed using the parameters of the system in Table 1 below:

Table 1. HMB Parameters

Symble	Value	Unit
m	2	kg
I_x=I_y	0.0067	kgm^2
I_z	0.0016	kgm^2
b	0.2	m
s	0.22	m
k_{as}=k_{bs}	-20368	N/m
k_{ai}=k_{bi}	28	N/A
P_{co}	50	Nm
P_{pa}	4x10^4	N/m
D_{co}	2	Nsm
D_{pa}	300	Ns/m
Ω	0-12000	RPM

4.1. The rotor is not rotating (Ω=0)

Case 1: Parallel mode

Initial state of the rotor deviates by a distance of -3x10^{-4} (m) from the x-direction and 1x10^{-4} (m) from the y-direction.

$$q_0 = \begin{bmatrix} 0 & -3\times10^{-4} & 0 & 1\times10^{-4} \end{bmatrix}^T$$

Simulation results in Fig.9.

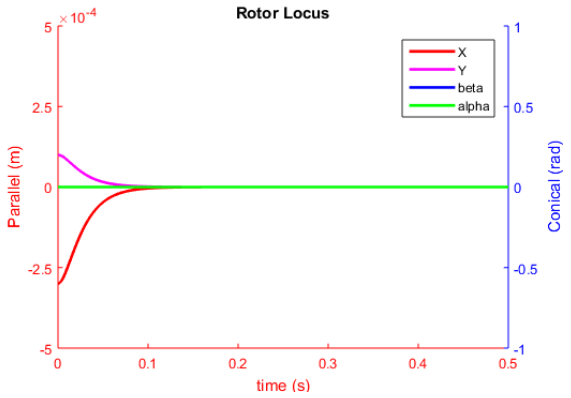

Fig. 9. The rotor locus is in parallel mode when the rotor is not rotating.

Case 2: Conical mode

Initial state of the rotor deviates from its rotation at angles of 5.23x10^{-3} (rad) in comparison to the y-direction and -8.72x10^{-3} (rad) to the x-direction.

$$q_0 = \begin{bmatrix} 5.23\times10^{-3} & 0 & -8.72\times10^{-3} & 0 \end{bmatrix}^T$$

Simulation results in Fig.10.

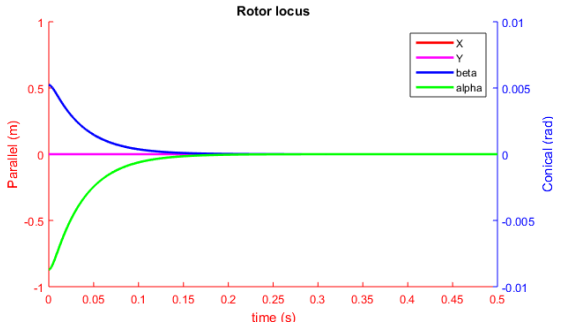

Fig. 10. The rotor locus is in conical mode when the rotor is not rotating

Case 3: Parallel / Conical mode

Initial state of the rotor deviates by a distance of -3x10^{-4} (m) from the x-direction and 1x10^{-4} (m) from the y-directions, rotation at angles of 5.23x10^{-3} (rad) in comparison to the y-direction and -8.72x10^{-3} (rad) to the x-direction.

Simulation results in Fig.11.

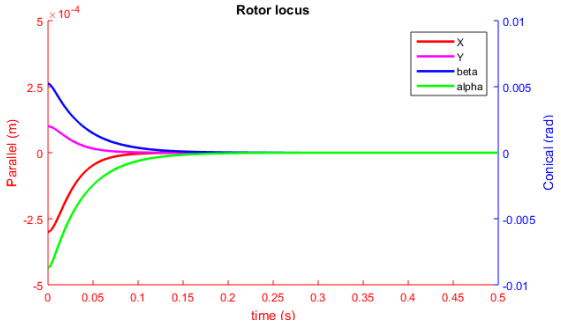

Fig. 11. The rotor locus is in parallel / conical mode when the rotor is not rotating.

Synthesize the moving trajectory of the center of Rotor in Fig.9 and Fig.10 by the moving trajectory of the center of Rotor in Fig.11. See that when the rotational speed of the Rotor (Ω=0), the displacement trajectory of the Rotor is divided into parallel mode and conical mode. Parallel/conical modes are completely independent of each other. This is true for the purpose when we design the controller.

4.2. The rotor is rotating (Ω≠0)

Case 1 : Ω=6000 rpm

Initial state of the rotor does not change compared with case 3 of part 4.1. The only difference is that the Rotor rotates with speed 6000 rpm.

$$q_0 = \begin{bmatrix} 5.23\times10^{-3} & -3\times10^{-4} & -8.72\times10^{-3} & 1\times10^{-4} \end{bmatrix}^T$$

Simulation results in Fig.12.

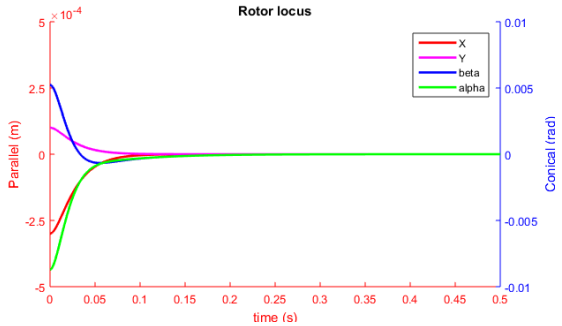

Fig. 12. The rotor locus is in parallel/conical mode with 6000 rpm.

Case 2: Ω=10500 rpm

Initial state is unchanged from above.

$$q_0 = \begin{bmatrix} 5.23\times10^{-3} & -3\times10^{-4} & -8.72\times10^{-3} & 1\times10^{-4} \end{bmatrix}^T$$

Simulation results in Fig.13.

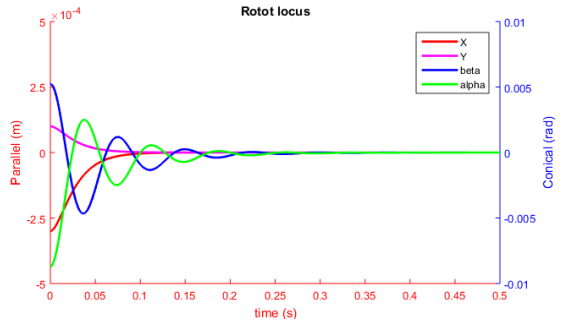

Fig. 13. The rotor locus is in parallel/ conical mode with 10500 rpm.

Look at the results in Figures 12 and 13, compare with the results in Figure 9,10,11 (the cases when Ω=0). We see that the parallel mode of the Rotor is unchanged, but the cone mode is changed with different rotation speed (Ω). It can be explained that the Rotor has been affected by the gyroscope phenomenon. However, we still achieve high control efficiency because the parallel/conical modes are still separated.

5. Conclusion

In this paper, the author has completed constructing a mathematical model for the novel hybrid active magnetic bearing. Using the equivalent magnetic circuit method to analyze and calculate the magnetic force of the magnetic poles acting on the rotor. The magnetic force is a nonlinear quantity that depends on the air gap and the current in the coil. But in the working domain with a very small change of air gap along with a small change in the corresponding control currents of the magnetic bearing, the magnetic force can be linearized and from there, a general linear equation of the HMBs. This equation consists of alternating the parallel motion and the conical motion of the rotor.

The next section, through the steps of transforming the mathematical matrix, the author has designed the PD controller with the goal of separating the movement of the Rotor into two separate parallel / conical modes. Finally, the simulation results showed that the PD centralized controller responded very well to the novel hybrid magnetic bearing. In particular, with this control method, the gyroscope effect of the rigid rotor did not negatively affect the parallel control process because it was separated.

References

[1] V. Babuska, S.M. Beatty, B.J. DeBlonk, et al., A review of technology developments in flywheel attitude control and energy transmission systems, in: Proceedings of the IEEE Aerospace Conference, vol. 4, March 2004, pp. 2784–2800.

[2] J.M.D. Coey., Permanent magnet applications, in: Journal of Magnetism and Magnetic Materials (2002) 441–456.

[3] T. Ohji, S. Ichiyama, K. Amei, et al., A new conveyor system based on a passive magnetic levitation unit having repulsive-type magnetic bearings, in: Journal of Magnetism and Magnetic Materials (2004) e1731–e1733.

[4] A. Hamler, V. Gorican, B. Stumberger, et al., Passive magnetic bearing, in: Journal of Magnetism and Magnetic Materials (2004) 2379–2380.

[5] R.B. Zmood, L.J. Qin, J.A. Kirk, et al., A magnetic bearing system design methodology and its application to a 50 Wh open core composite flywheel, in: Proceedings of the Energy Conversion Engineering Conference 32nd Intersociety, vol. 27 (4), August 1997, pp. 2306–2311.

[6] Alexei V. Filatov, Patrick T. McMullen, Lanvence A. Hawking, et al., Magnetic bearing actuator design for a gas expander generator, in: Proceedings of the Ninth International Symposium on Magnetic Bearings, Lexington Kentucky, USA, pp. 81–86, August 3–6, 2004.

[7] Brian T. Murphy, Hamid Ouroua, Matthew T. Caprio, John D. Herbst., Permanent magnet bias, homopolar magnetic bearings for a 130 kW-hr composite flywheel, in: Proceedings of the Ninth International Symposium on Magnetic Bearings, Lexingtong Kentucky, USA, pp. 66–72, August 3–6 2004.

[8] Xu. Yanliang, Dun. Yueqin, Wang. Xiuhe, et al., Analysis of hybrid magnetic bearing with a permanent magnet in the rotor by FEM, in: IEEE Transactions on Magnetics 42 (4) (2006) 1363–1366.

[9] H. Bleuler., Decentralized Control of Magnetic Rotor Bearing Systems, in: PhD thesis, No. 7573, Federal Institute of Technology (ETH), Z¨ urich, Switzerland, 1984.

[10] J.C. Doyle., Guaranteed margins for LQG regulators, in: IEEE Transactions on Automatic Control, AC-23(4):756–757, August 1978.

[11] Tian Ye, Sun Yanhua, Yu Lie., LQG Control of Hybrid Foil-Magnetic Bearing, in: 12th International Symposium on Magnetic Bearings, 2010.

[12] G. J. Balas, J. C. Doyle, K. Glover, A. K. Packard, and R. Smith., μ Analysis and Synthesis Toolbox User's Guide, in: The MathWorks, Natick, MA, 1995.

[13] F. Matsumura, T. Namerikawa, K. Hagiwara and M. Fujita., Application of Gain Scheduled H∞ Robust Controllers to a Magnetic Bearing, in: IEEE Trans. Control Systems Technology, vol. 4, no. 5, pp. 484-493, 1996.

[14] Amin Noshadi, Juan Shi, WeeSit Lee, Peng Shi, Akhtar Kalam., High performance H∞ control of non-minimum phase Active Magnetic Bearing system, in: IECON 2014 - 40th Annual Conference of the IEEE Industrial Electronics Society.